PCCP

Accepted Manuscript

ROYAL SOCIETY OF CHEMISTRY

www.rsc.org/pccp

PCCP

RSCPublishing

ARTICLE

Spectral evidence for hydrogen-induced reversible segregation of CO adsorbed on titania-supported rhodium

Cite this: DOI: 10.1039/x0xx00000x

D. Panayotov,*[a] M. Mihaylov,[a] D. Nihtianova,[ac] T. Spassov,[b] and K. Hadjiivanov*[a]

Reduction of a 1.3 % Rh/TiO_2 sample with carbon monoxide leads to formation of uniform Rh nanoparticles with a mean diameter $d_p \approx 2.2$ nm. Adsorption of CO on the reduced Rh/TiO_2 produces linear and bridged carbonyls bound to metallic Rh^0 sites and only few geminal dicarbonyls of Rh^I. The ν(CO) of linear Rh^0–CO complexes is strongly coverage dependent: it is observed at 2078 cm^{-1} at full coverage and at ca. 2025 cm^{-1} at approximated zero coverage. At low coverage, this shift is mainly caused by dipole-dipole interaction between the adsorbed CO molecules while at high coverage the chemical shift also becomes important. Hydrogen hardly affects the CO adlayer at high CO coverages. However, on partially CO–covered surface ($\theta_{CO} \approx 0.5$) adsorption of H_2 at increasing pressure leads to a gradual shift of the band of linear Rh^0–CO from 2041 to 2062 cm^{-1}. Subsequent evacuation almost restores the original spectrum demonstrating the reversibility of the hydrogen effect. By the use of ^{12}CO + ^{13}CO isotopic mixtures it is established that addition of hydrogen to the CO–Rh/TiO_2 system leads to increase in the dynamic interaction between the adsorbed CO molecules. This evidences increase of the density of the adsorbed CO molecules and indicates segregation of the CO and hydrogen adlayers. When CO is adsorbed on hydrogen-precovered surface, the carbonyl band maximum is practically coverage independent and is observed at 2175-2173 cm^{-1}. These results are explained by a model according to which CO successively occupies different rhodium nanoparticles.

Received 00th January 2014,
Accepted 00th January 2014

DOI: 10.1039/x0xx00000x

www.rsc.org/

1. Introduction

Vibrational spectroscopy of adsorbed CO is among the most used and powerful methods for identification of active sites and elementary mechanistic steps in heterogeneous catalytic reactions proceeding on the surfaces of both single crystal and supported metals.[1] The spectral performance of adsorbed CO is determined by different factors: geometry of bonding, nature of the bond and the coverage.[1-3] For linearly bonded CO the position of the carbonyl band depends mainly on the balance between the σ- and π-bonds.[3-6] The σ-bonding leads to an increase in ν(CO), while the π-bonding causes the opposite effect.[3] With metal surfaces the π-bonding usually predominates and, as a result, ν(CO) is detected below the CO gas-phase stretching frequency (2143 cm^{-1}). When CO bridges two metal atoms rehybridization to sp^2 hybrid orbitals occurs which leads to lower C-O bond order and ν(CO) is shifted to 2000-1880 cm^{-1}. Multi-centered carbonyls formed on three-fold and four-fold hollow sites are observed at even lower wavenumbers (below ~ 1880 cm^{-1}).[7]

The position of ν(CO) of linear carbonyls is primarily affected by the coordination state of the adsorption site. The lower its coordination number, the greater the adsorption strength is and thus the frequency of ν(CO) mode normally appears at lower wavenumbers. Note that low coordinated atoms on edges, corners and defects are likely to represent a large proportion of all the available adsorption sites on small particles.[5,6,8]

Usually, the position of the carbonyl bands is coverage dependent. For most metal surfaces, ν(CO) of linearly adsorbed CO is blue shifted with the increase of coverage. This shift is mainly caused by the cooperative effect of two phenomena: (i) dipole-dipole coupling between the adsorbed molecules (dynamic shift) and (ii) competition between adsorbate molecules for electrons back donated from the metal to form π–bonds (chemical shift).[3]

Rhodium is an important component in many catalysts for CO conversion, e.g. selective CO hydrogenation,[9, 10] reduction of NO by CO in automotive exhaust gas,[11, 12] hydroformylation

reaction (aldehyde production from olefins, carbon monoxide, and hydrogen),[13, 14] etc. The Rh/TiO_2 system is well known as a Fischer-Tropsch catalyst,[15] where the details on the CO and H_2 adsorption and coadsorption have fundamental importance.

There are many studies of CO and H_2 adsorption and coadsorption on rhodium single crystals. On both Rh(111) and Rh(100) planes CO forms coverage dependent ordered structures consisting of linear (on top) and bridge–bound species.[16-21] Twofold bridge-bound CO has been observed on Rh(100) surface[22] while CO bound at threefold bridge (hollow sites) sites is characteristic for Rh(111) surface.[17] Hydrogen adsorbs dissociatively on both Rh(111)[23] and Rh(100)[24] surfaces (at ~ 100 K), and forms no ordered structures observable by LEED. Co-adsorbed CO and hydrogen are found to segregate on the close packed Rh(111) surface.[25] On the more open Rh(100) surface, CO and hydrogen adsorbates segregate when CO is preadsorbed, whereas a mixed adlayer is formed when H_2 is adsorbed first.[18,24]

The chemistry of CO adsorbed on supported rhodium catalysts is different. Numerous studies have shown that CO provokes oxidative disruption of supported metal rhodium particles forming isolated rhodium(I) gem dicarbonyls[26,27] The disruption of Rh crystallites is assisted by surface hydroxyl groups[28-30] or surface defects[31,32] of the oxide support. The effect of hydrogen on CO preadsorbed on oxide supported rhodium has also been studied.[9,29,33-35] However, most of these studies were focused on the interaction of H_2 with isolated geminal dicarbonyl species of Rh^I and the reverse aggregation of isolated Rh^I ions to metallic Rh crystallites.[28,29,36] Production of water during interaction of hydrogen with rhodium on reducible supports is additional factor that complicates the spectra as compared to the single crystal systems. Generally, detailed spectroscopic investigation of supported rhodium systems towards the effect of hydrogen on the adsorbed CO layer has not attracted the attention that has been paid when the effect was studied with single crystals. It is of definite interest to establish the phenomena occurring with supported metal nanoparticles because they are characteristic of the real Rh–metal oxide catalyst systems.

The aim of this work is to study the effect of hydrogen on the CO adsorbate layer formed on titania supported rhodium nanoparticles. To clarify the nature of this effect we used IR spectroscopy of adsorbed CO and a ^{13}CO–enriched ^{12}CO + ^{13}CO isotopic mixture.

2. Experimental

2.1. Sample preparation

The support used for the deposition of Rh nanoparticles was a commercially available Degussa P25 titanium dioxide material containing 80 % anatase and 20 % rutile.[37] The Rh/TiO_2 sample was prepared by incipient wetness impregnation of 1.0 g TiO_2 with 2.5 mL 1.4 wt % aqua solution of $RhCl_3.xH_2O$ (38.7% Rh, VEB Bergbau und Hüttenkombinat "Albert Funk") and dried at 373 K. The Rh/TiO_2 sample thus obtained contained, nominally, 1.3 wt % of rhodium. Before IR experiments, the sample was reduced *in situ* in the IR cell by CO as described below. For the TEM analysis reduced Rh/TiO_2 sample was passivated by successive addition of small doses of oxygen *in situ* in the IR cell before exposing to air and transferring into the TEM equipment.

2.2. Techniques

FTIR spectra were recorded at ambient temperature with a Nicolet Avatar 360 FTIR spectrometer accumulating 64 scans at a spectral resolution of 2 cm^{-1}. Self–supporting pellets (ca. 10 mg cm^{-2}) were prepared from the sample powder and treated directly in a purpose-made IR cell. The cell was connected to a vacuum-adsorption apparatus with a residual pressure below 10^{-3} Pa. Prior to the adsorption experiments, the sample was first oxidized (15.0 kPa O_2, 673 K, 30 min), evacuated at 523 K for 2 min and then cooled to 298 K under dynamic vacuum. After that, the sample was reduced by exposure to 4.0 kPa CO at 523 K for 1 min and then evacuated at 298 K. The CO coverage measured by the integrated IR absorbance of rhodium carbonyls under these conditions was adopted as the saturation CO coverage of exposed Rh sites. Partial CO coverages were obtained by evacuation of CO-saturated Rh/TiO_2 at chosen elevated temperatures. Liquid nitrogen trap served to remove traces of water vapour from the cell during the experiments.

Carbon monoxide (> 99.5 % purity) was supplied by Merck and labelled carbon monoxide ^{13}CO (99 atom % ^{13}C, <5 atom % ^{18}O), by ISOTEC. Oxygen (> 99.999%) and hydrogen (> 99.999%) were both purchased from Messer. All gases (CO, CO isotopic mixture, O_2 and H_2) were additionally purified by passing through a liquid nitrogen trap.

The histogram of the metal particle size has been obtained by counting about 300 particles.

3. Results

3.1. Sample characterization by TEM

The TEM study was performed with an *ex-situ* CO-reduced Rh/TiO_2 sample. The low-magnification TEM images (Fig. 1 A, B) revealed that TiO_2 particles (average size 25 nm) are decorated by Rh nanoparticles. The recorded one- and two-dimensional HRTEM images confirmed the phase composition of the TiO_2 support.

The histogram in Fig. 1 C shows a rather narrow size distribution of Rh particles with mean diameter $d_p \approx 2.2$ nm. An estimate showed that Rh nanoparticles are pseudo-hemispherical and possess an aspect ratio (height/diameter) of ~ 0.3–0.4. Lattice fringes (100) and (111) of rhodium particles are also registered. Moreover, lattice fringes (100) of anatase coexist with (100) lattice fringes of rhodium (Fig. 1 D) while lattice fringes (101) of anatase TiO_2 coexist with (111) lattice fringes of rhodium (Fig. 1 E). These data suggest that Rh nanoparticles with different exposed faces preferentially grow on different TiO_2 crystal planes.

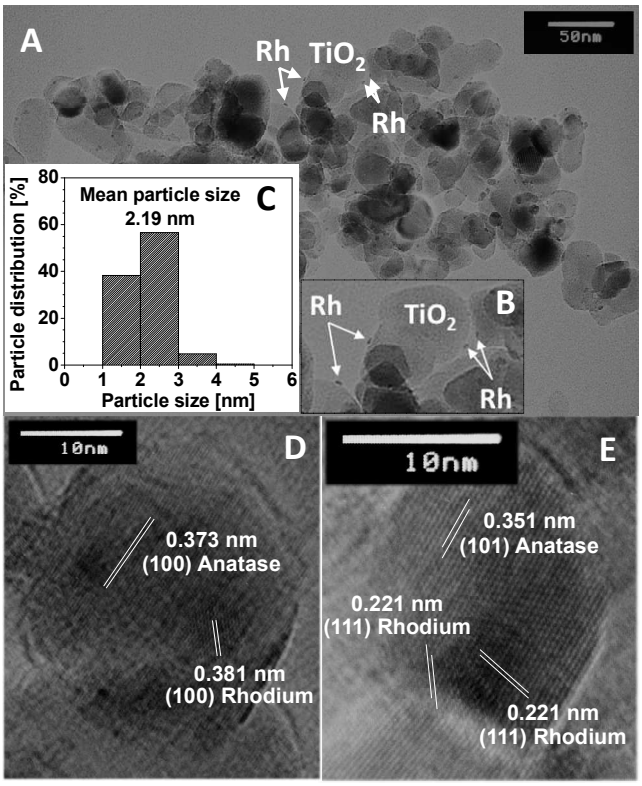

Figure 1. (A) Bright field TEM image of the 1.3 wt. % Rh/TiO_2 sample; (B) An enlarged view of small Rh particles at the surface of TiO_2; (C) A histogram of the apparent diameter of Rh particles; (D) and (E) HRTEM images of ~ 25 nm anatase particles bearing ~ 2–3 nm Rh particles.

3.2. Adsorption of CO

The IR spectrum of CO (4 kPa equilibrium pressure) adsorbed at 298 K on the CO–reduced Rh/TiO_2 sample exhibits two sharp bands at 2187 and 2078 cm^{-1} and a broad feature centered at 1870 cm^{-1} (Fig. 2 A, spectrum *a*). The band at 2187 cm^{-1} is observed only in the presence of gas-phase CO and arises from CO bound to low–coordinated Ti^{4+} sites on the TiO_2 support.[38] The intense band at 2078 cm^{-1} is unambiguously assigned to linear Rh^0–CO species while the broad band at ~1870 cm^{-1} is attributed to bridged carbonyls formed on Rh nano-particles.[8,36,38]

The sample was evacuated at ambient and elevated temperatures (Fig. 2A spectra *b–j*). This resulted in a fast disappearance of the Ti^{4+}–CO band at 2187 cm^{-1}. The principal Rh^0–CO carbonyl band decreased in intensity and was gradually shifted from 2078 cm^{-1} to 2026 cm^{-1}. The dependence of the band position on the coverage is shown on Fig. 2B. The measured shift in ν(CO) was Δν(CO) = 52 cm^{-1} for CO coverage (θ_{CO}) change from ~ 1 to ~ 0.04.[8]

Computer treatment indicates a good approximation of the spectrum when the band of Rh^0–CO carbonyls was deconvoluted into three components (see Fig. S1 of the Supporting Information†). These components could be

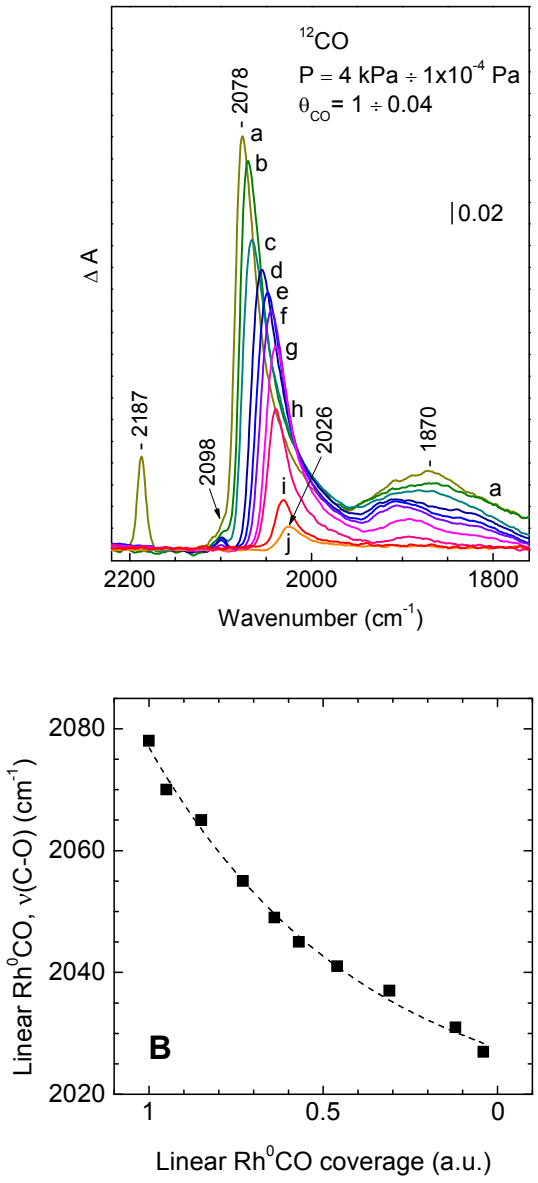

Figure 2. Panel (A): FTIR spectra of CO adsorbed at 298 K on CO–reduced Rh/TiO_2. Equilibrium CO pressure of 4 kPa, spectrum *a*; evacuation at 298 K, *b*; and, sequential 10 min evacuations at 448 K (c–h) and at 523 K (i–j). The spectra are background corrected. Panel (B): Dependence of ν(CO) of Rh^0–CO species on the relative CO coverage. The dash line is a guide for the eye.

attributed to CO bound to Rh sites having different coordination.[5,8,39] For small Rh particles with mean size 2–3 nm, the fraction of low–coordinated Rh sites at edge, step and corner positions may account for ~50 % of the total number of exposed rhodium.[8] Unfortunately, it is difficult to estimate the fraction of various Rh sites from the IR spectra because of intensity transfer phenomena usually observed with CO adsorbed on metal surfaces.[5,40,41]

The changes in the region of bridging carbonyls are more complex: the broad band consists of at least two main components. These features show different stability and the high-frequency component tends to red shift with decreasing coverage. Based on previous assignment,[8] bands in the 1910 – 1890 cm^{-1} region can be attributed to twofold bridge–bound CO while bands in the 1870 – 1820 cm^{-1} region, to CO bound to three-fold hollow sites.

After evacuation at 298 K (Fig. 2A, spectrum *b*) a weak band at 2098 cm^{-1} becomes observable and is better discernible after a short evacuation at 448 K (Fig. 2A, spectrum *c*). This band is attributed to the symmetric modes of isolated $Rh^{I}(CO)_2$ geminal species,[28,29,36,38] the respective antisymmetric modes being masked by the intense carbonyl band of the Rh^{0}–CO species.[29,36,38] The 2098 cm^{-1} band declined under dynamic vacuum at elevated temperatures and vanished at 523 K. The position of the band was not affected by the coverage. Such behavior is consistent with the proposed assignment as far as the two CO ligands in the geminal species do not participate in dipole–dipole interactions.[29,36] Separate experiments have revealed that the fraction of the geminal dicarbonyls is much more important with hydrogen-reduced sample (Fig. S2, spectrum *b*), in line with literature reports.[36,38] $Rh^{I}(CO)_2$ species were the principal carbonyls produced after CO adsorption on oxidized Rh particles, after exposure to O_2. In the latter case, however, some carbonates were produced after CO adsorption. The results evidence that the reduction with CO ensures that rhodium remains mainly in metallic state in the presence CO at 298 K.

After evacuation at 523 K, re–adsorption of CO (4 kPa) at 298 K practically reproduced the spectrum of CO–saturated sample (shown on Fig. 2A, spectrum *a*), evidencing that no irreversible changes occurred with the Rh particles during the experiments.

3.3. Adsorption of H_2

To obtain clean surface, the reduced sample was evacuated at 548 K for 20 min. This procedure ensured disappearance of all carbonyl bands. Exposure of the sample to H_2 gas at 298 K led to immediate raise in the IR background absorbance as shown in Fig. S3. The observed IR absorbance is featureless and increases exponentially from ~ 4000 to 1000 cm^{-1}. It is attributed to delocalized conduction band electrons that accumulate in TiO_2 with the H_2 exposure. Similar observations were recently reported for H_2 adsorption on Au/TiO_2.[42] The results evidence that H_2 dissociates on the metallic Rh particles and produces atomic hydrogen that spillover on the TiO_2 support. The H atoms protonate surface oxygen atoms to OH groups while injecting electrons into the conduction band of TiO_2.[15,42] These observations are consistent with literature data on H_2 adsorption on rhodium monocrystals where H_2 was found to dissociate. More details on the sample interaction with H_2 are presented in the Supporting Information.

3.4. Adsorption of CO on hydrogen pre-covered sample

The next experiments were designed to check the effect of pre-adsorbed hydrogen on the adsorption of CO. Before the H_2 exposure, the CO-reduced Rh/TiO_2 sample was first evacuated at 548 K for 20 min and then cooled down to 298 K under dynamic vacuum. Then hydrogen (4 kPa equilibrium pressure) was introduced to the sample and small portions of CO were successively added to the system to increase the CO coverage, as shown in Fig. 3. The Rh^{0}–CO band appeared at 2073 cm^{-1} for θ_{CO} = 0.27 and its position changed only slightly with the coverage, reaching the value of 2075 cm^{-1} for θ_{CO} = 0.67. Note that this value is very close to the value observed for full CO coverage in the absence of hydrogen (Fig. 2A, spectrum *a*). The band of bridging carbonyls that appeared at ca. 1900 cm^{-1} was expressed even at low coverages. As seen from the inset in Fig. 3, where normalized spectra are presented, the relative intensity of bands due to linear and bridge species remains the same at different CO coverages. The observations that under H_2 equilibrium pressure the ratio liner/bridging carbonyls as well as the positions of the carbonyl bands remain constant with CO coverage can be rationalized by assuming that, in the presence of pre-adsorbed hydrogen, even small amounts of adsorbed CO form adlayer with high density of CO molecules. In this CO adlayer, the interaction between CO oscillators is similar to that in the CO-saturated layer on the hydrogen-free surface.

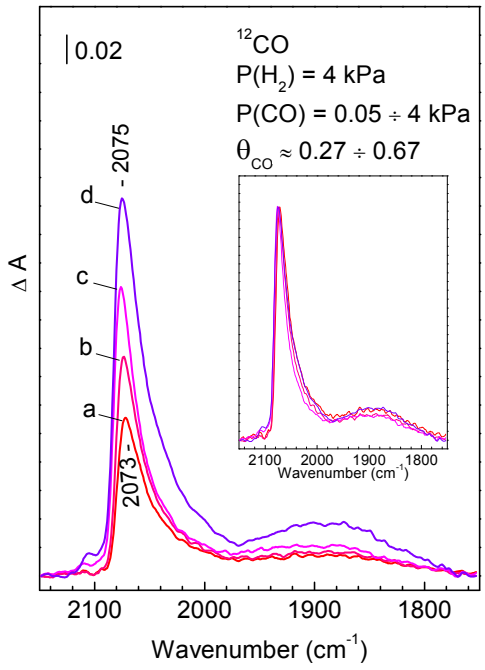

Figure 3. FTIR spectra of CO adsorbed at 298 K on H_2–precovered Rh/TiO_2 sample. The sample was then exposed to H_2 (4 kPa equilibrium pressure) and small portions of CO were added at 298 K (*a*–*d*). The spectra are background corrected. The inset shows the same spectra normalized according to the intensity of the band at 2075-2073 cm^{-1}.

This supposition is confirmed by the computer treatment of the spectra for linear Rh^0–CO species which revealed a good approximation when the bands were deconvoluted into three components with positions similar to the positions observed with full CO coverage in absence of hydrogen (see Fig. S4).

3.5. Effect of hydrogen on pre-adsorbed CO

First series of experiments were performed with a Rh/TiO_2 sample that was saturated with CO and then evacuated at 298 K. Just before the admission of H_2, the spectrum of the sample exhibited a band at 2066 cm^{-1} due to linearly bound Rh^0–CO species and the estimated θ_{CO} was 0.87 (Fig. S5, spectrum *a*). At this high CO coverage, the effect of H_2 admission on the carbonyl bands was practically negligible: after 60 min exposure to hydrogen, the band at 2066 cm^{-1} due to Rh^0–CO species was slightly blue shifted, to 2069 cm^{-1} (Fig. S5, spectrum *b*). Upon evacuation, this band appeared at 2063 cm^{-1} (Fig. S5, spectrum *c*), i.e. at slightly lower frequency than that registered before H_2 exposure. This small difference is attributed to desorption of some CO during evacuation. Thus, the results evidence that hydrogen hardly affects preadsorbed CO when the CO coverage is relatively high.

The next series of experiments with co-adsorbed H_2 were performed at partial CO coverage, i.e. at θ_{CO} = 0.48, that was achieved after 50 min evacuation of the CO-saturated sample at 448 K.

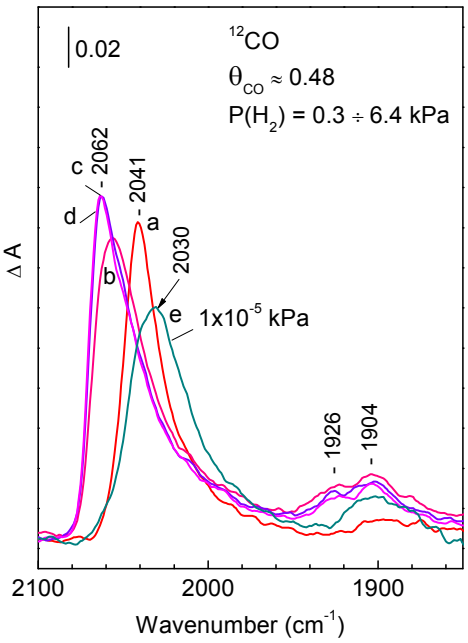

Figure 4. FTIR spectra of adsorbed CO during a CO + H_2 co-adsorption experiment carried out at 298 K with Rh/TiO_2 that contained partial CO coverage, i.e. θ_{CO} = 0.48. Adsorption of CO (4 kPa), followed by 1 min evacuation at 473 K (a), introduction of H_2 to the system at equilibrium pressures of 0.5 (b), 4.0 (c) and 6.4 (d) kPa, and, after evacuation at 1 × 10^{-5} kPa (e). The spectra are background corrected.

The IR spectrum registered before H_2 admission (Fig. 4, spectrum *a*) was featured mainly by one Rh^0–CO band positioned at 2041 cm^{-1}. Only a very weak feature around 1900 cm^{-1} was detected in the region of bridging carbonyls evidencing that CO was essentially adsorbed in linear form. Additions of hydrogen to the system, at progressively increasing H_2 pressure from 0 to 4 kPa, led to a gradual blue shift of the band due to linear Rh^0–CO species up to 2062 cm^{-1} (Fig. 4, spectra *a*–*c*). Concomitantly, a doublet with resolved maxima at 1926 and 1904 cm^{-1} due to bridging CO species developed. Note that in the absence of hydrogen, bridging CO is rather typical of high CO coverage.

Further increase of hydrogen pressure to 6.4 kPa (Fig. 4, spectrum *d*) hardly affected the carbonyl bands. Computer treatment of the spectra for linear Rh^0–CO species revealed again a good approximation when the Rh^0–CO bands were deconvoluted into three components (Fig. S6 A, B). Subsequent evacuation of the sample (Fig. 4, spectrum *e*) almost restored the original spectrum of CO–Rh/TiO_2: the band of linear Rh^0–CO species was back red shifted to ca. 2030 cm^{-1} and was slightly broadened but its integral intensity remained the same; the 1926 cm^{-1} band of bridged carbonyls disappeared while that at 1904 cm^{-1} decreased in intensity.

Another effect of hydrogen addition was the formation of small amount of adsorbed water as evidenced by a band that appeared at 1618 cm^{-1} (not shown). These traces of water are produced by reduction of residual oxidized rhodium species and/or of TiO_2 support by H atoms produced by H_2 dissociation on Rh. The band at 1618 cm^{-1} resisted evacuation at ambient temperature. Evidently, the presence of water led to small red shift of the carbonyl bands (compare spectra *a* and *e* from Fig. 4). A similar effect has been reported for water-CO coadsorption on a Pt/TiO_2 sample.[43]

The observation of practically reversible blue shift in the frequency of Rh^0–CO band induced by H_2 co-adsorption, as shown in Fig. 4, provides a spectral evidence that hydrogen adsorption causes reversible changes in the CO adsorption layer. The results strongly suggest hydrogen-induced segregation of the CO adsorption layer.

3.6. Experiments involving ^{12}CO + ^{13}CO isotopic mixture

In order to confirm the hypothesis about the segregation of CO and hydrogen adlayers we performed experiments involving a ^{12}CO + ^{13}CO isotopic mixture enriched to ^{13}CO. The experiments aimed at estimating the dynamic coupling of CO molecules when adsorbed either alone or co-adsorbed with hydrogen. In order dynamic interaction to occur, the adsorbed molecules must: (i) be adsorbed on one plane and close each to other, (ii) be parallel and (iii) vibrate with the same intrinsic frequency.[3,44] Thus, the dynamic interaction will increase at increasing density of molecules due to the enhanced vibrational coupling of adsorbed dipole molecules.[3,44,45] The requirement the molecules to vibrate with the same frequency is the basis of

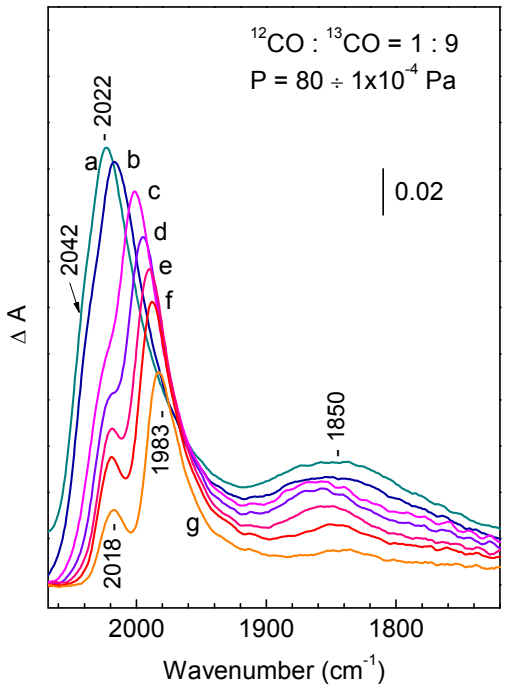

Figure 5. FTIR spectra of ^{12}CO + ^{13}CO isotopic mixture (1 : 9 molar ratio) adsorbed at 298 K on CO-reduced Rh/TiO_2. Equilibrium CO pressure of 80 Pa (a); evacuation at 298 K (b), and at 448 K for increasing time (c – g).

the experimental determination of the dynamic frequency shift.[44] If a ^{12}CO molecule is surrounded by isotopically labelled ^{13}CO molecules, it will not be involved in dynamic interactions. Therefore, the difference between the frequency $\nu_i(^{12}CO)$, observed after adsorption of ^{12}CO, and the frequency $\nu_{ii}(^{12}CO)$, obtained with isotopic ^{12}CO + ^{13}CO mixture containing small amount of ^{12}CO, will be equal to the value of the dynamic shift, i.e. $\Delta\nu_{dyn} = \nu_i(^{12}CO) - \nu_{ii}(^{12}CO)$.

The Rh/TiO_2 sample was reduced by exposure to a ^{12}CO + ^{13}CO mixture (with an 1 : 9 molar ratio) at 523 K. The spectrum of reduced Rh/TiO_2 sample contacted with the ^{12}CO + ^{13}CO mixture at equilibrium pressure of 80 Pa (Fig. 5, spectrum *a*) exhibits an intense IR band at 2022 cm^{-1} and a broad feature around 1850 cm^{-1}. These two bands are assigned to Rh^0–^{13}CO and Rh^0–(^{13}CO)–Rh^0 complexes, respectively. In addition, the band at 2022 cm^{-1} has a shoulder at 2042 cm^{-1} (the exact band position was obtained from the second derivative of the spectrum).

When CO coverage was reduced by evacuation at increasing temperatures (Fig. 5, spectra b – g), the 2022 cm^{-1} band and its satellite at 2042 cm^{-1} decreased in intensity and shifted to lower frequencies. Simultaneously, the shoulder was gradually converted into a separate band. Prolonged evacuation at 448 K resulted in two well resolved bands at 2018 and 1983 cm^{-1} (Fig. 5, spectrum g). The band at 2018 cm^{-1} is assigned to Rh^0–^{12}CO species. Because of the increase of the dynamic interaction between adsorbed ^{13}CO molecules at high coverage,

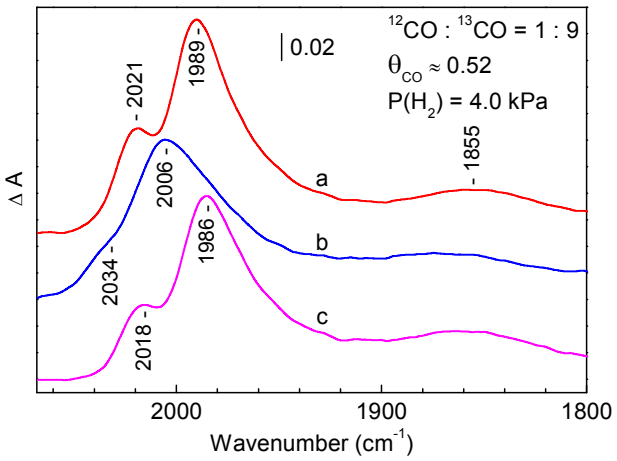

Figure 6. FTIR spectra of ^{12}CO + ^{13}CO isotopic mixture (1 : 9 molar ratio) adsorbed at 298 K on CO-reduced Rh/TiO_2: after evacuation at 484 K for 20 min (a); after interaction with 4 kPa H_2 at 298 K(b) and after evacuation at 298 K (c).

the Rh^0–^{13}CO band is strongly shifted to high frequencies thus approaching the value of the Rh^0–^{12}CO band.

Let first consider the spectra at low coverage (Fig. 5, spectra d-g). It is seen that, in this series of spectra, the Rh^0–^{12}CO band is practically coverage independent. This means that no measurable chemical shift of the band occurs at low coverage, which is consistent with the results reported by Linke et al.[17] These authors concluded that on Rh(111) surface at coverage up to 0.5 ML, all frequency shifts are due to dipole–dipole coupling while at larger coverages ($\theta_{CO} > 0.5$) some chemical effects start to contribute.

At coverage of 0.33 the Rh^0–^{13}CO band was detected at 1983 cm^{-1} (Fig. 5, spectrum *g*). Considering the ^{12}CO/^{13}CO isotopic shift factor (0.97777)^3 one can easily derive the expected position of the corresponding ^{12}CO modes (i.e. 2028 cm^{-1}) if the ^{12}CO molecules were involved in dynamic interaction as the ^{13}CO molecules. However, the experimentally observed ^{12}CO band (in ^{13}CO surrounding) was at 2018 cm^{-1}, i.e. the dynamic shift amounts to 10 cm^{-1} at this CO coverage. Using the same approach, the dynamic shift was calculated to increase to 17 cm^{-1} at coverage of ≈ 0.58. (Fig. 5, spectrum *e*).

At higher coverages (Fig. 5, spectra *a, b*) the chemical shift substantially contributed to the position of the carbonyl bands as evidenced by the substantial blue shift of the band around 2020 cm^{-1}. Irrespective of this phenomenon, the dynamic interaction could be calculated using the same approach. Thus, for the highest coverage ($\theta \approx 1$) it was found to be 26 cm^{-1} (Fig. 5, spectrum *a*), i.e. about half of the total shift. Indeed, it is expected that the dynamic shift will decrease with CO coverage reaching zero when a single CO molecule is adsorbed, as shown in Fig. S7. Note that, due to superimposition of the bands, we were able to calculate the dynamic shift only for the main component of the carbonyl band.

Consider now the interaction of hydrogen with preadsorbed isotopic mixture as shown in Fig. 6.

An initial CO coverage of θ_{CO} = 0.52 was obtained by evacuation of preadsorbed CO isotopic mixture at 484 K for 20 min (Fig. 6, spectrum *a*). At this coverage the dynamic shift was calculated to be 13 cm^{-1}. Subsequent introduction of hydrogen (Fig. 6, spectrum *b*) resulted in a blue shift of the Rh^0–^{12}CO and Rh^0–^{13}CO bands. However, the shift was much more pronounced with the ^{13}CO band. Calculations showed that in the presence of hydrogen the dynamic shift increased to 18 cm^{-1}.

As already noted, some H_2O was produced after hydrogen submission and was not removed by subsequent evacuation. Thus, the most correct way to estimate the effect of hydrogen is to compare the spectra before and after evacuation of hydrogen. After evacuation of the sample the dynamic shift dropped to 13 cm^{-1}, the value obtained before hydrogen adsorption. Thus, it appears that, although water traces slightly affects the carbonyl spectra, it practically does not influence the dynamic interaction between the adsorbed CO molecules.

4. Discussion

4.1. Adsorption of CO

The results of this study clearly show that reduction of Rh/TiO_2 in CO atmosphere at 523 K produces rhodium nanoparticles exposing mostly metallic Rh sites that at room temperature adsorb CO molecules as linear "on top" species and bridged structures; only very limited number of isolated $Rh^I(CO)_2$ species were formed. In contrast, reduction of Rh/TiO_2 in H_2 atmosphere at the same temperature produced Rh nanoparticles that are disrupted upon adsorption of CO at 298 K to form isolated $Rh^I(CO)_2$ species (Fig. S2), in consistence with previous reports.[36,38] A possible explanation is that the reduction of Rh/TiO_2 with H_2 probably produces Rh particles with rough surfaces that are easily disrupted upon adsorption of CO. In opposite, reduction of Rh/TiO_2 with CO likely produces metallic Rh nanoparticles with smooth surface that are stable towards oxidative disruption in CO atmosphere. This point of view is supported by the TEM photographs showing exposed (100) and (111) rhodium crystal planes on the rhodium nanoparticles (See Fig. 1).

The spectrum of CO adsorbed on our CO-reduced sample is dominated by the band of linearly bound carbonyl species. The maximum of this band is strongly coverage dependent and indicative of CO coverage. The experiments with ^{12}CO + ^{13}CO isotopic mixture (Fig. 5) indicated that at low coverages the shift is essentially caused by dipole–dipole coupling of adsorbed CO molecules. This coupling also largely contributes to the shift occurring at higher coverages.

Bridging CO is rather typical of high CO coverage. Based on previous studies with single crystal[17,18] and nanoparticulate Rh,[8] the broad complex band in the region of bridging carbonyls with maxima appearing in the regions ~ 1910 – 1890 cm^{-1} and 1870 – 1820 cm^{-1} are assigned to CO bound at two-fold bridge sites exposed on Rh(100)[18] facets and three-fold hollow sites on more compact Rh(111)[17] facets, respectively.

According to TEM analysis, the supported Rh nanoparticles have a rather narrow size distribution, as shown in the histogram of Fig. 1C. Thus, it might be suggested that the asymmetric broadening of the band of linear CO species to the low frequency side is not associated with a substantially broad distribution of Rh particles sizes on the Rh/TiO_2 sample. Rather, the band broadening for linear species is related to the population of Rh sites with different coordination, as previously suggested for supported metal nano-particles exposing both well–coordinated Rh sites (at Rh crystal planes) and low–coordinated Rh sites (at steps, edges and corners).[8,39,46] Here, as already mentioned, one should take into account the possible intensity transfer. Based only on the deconvolution of CO spectra of the linearly bound CO species obtained at different coverages (Fig. S1), it is impossible to assign directly the deconvoluted spectral components to the vibrations of CO adsorbed at different types of Rh sites (corner, edge, plane), as far as these spectral features are not well-resolved with coverage, as in the case of Pt/SiO_2.[39,46]

4.2. Adsorption of H_2 and co-adsorption of CO and H_2

Hydrogen adsorbs dissociatively on both Rh(111) and Rh(100) single crystal surfaces even at 100 K where H atoms occupy hollow sites.[23,24,47] Dissociative adsorption of hydrogen on Rh nanoparticles supported on TiO_2 has been observed at room temperature.[48] In our IR study of H_2 interaction with Rh/TiO_2 sample at 298 K we have observed an increase in the IR background absorbance as shown in Fig. S3. Dissociation of H_2 on metallic particles produces H atoms that can spillover onto TiO_2 support where they protonate the surface while injecting electrons into the conduction band of TiO_2.[42,48]

When CO doses were adsorbed in presence of hydrogen, the CO molecules formed highly compressed CO adlayer with spectral characteristics typical of CO-saturated sample in absence of hydrogen. These observations indicate that CO successively saturates separate rhodium nanoparticles replacing adsorbed hydrogen. Small deviations of this model are responsible for slight variation of the CO frequency at different coverages (Fig. 4). These results differ from the findings with monocrystals where formation of mixed CO-hydrogen layers were observed for (100) Rh plane even at 150 K.[18,20]

The results on hydrogen adsorption on sample pre-covered by CO also indicate H_2-induced changes in the density of CO adlayer resulting in a substantial shift in the CO stretching frequencies. The structure of the CO adlayer on monocrystal surfaces strongly depends on the presence of co-adsorbed hydrogen. When CO is adsorbed first, the H atoms incoming to CO adlayer repel the nearby CO molecules that move away to reduce the repulsive interaction and thus the CO and H adlayers are segregated.[20,24,25,49]

When hydrogen was exposed to Rh nanoparticles highly saturated with CO ($\theta_{CO} \approx 0.87$, Fig. S2) no measurable changes in the vibrational spectra of both linear and bridge–bound CO

species were detected. These results were expectable, as far as no significant further compression of CO adlayer was possible. However, when hydrogen was exposed to Rh nanoparticles partially covered with CO ($\theta_{CO} \approx 0.48$, Fig. 2), a blue shift in the frequency of linear CO species was observed, signalling the compression of CO adlayer.

The observed H_2-induced changes in the values of the dynamic shift for a given total CO coverage could be explained only by the change of the density of the adsorbed CO molecules. Therefore, the results of the ^{12}CO + ^{13}CO co-adsorption experiments strongly support the hypothesis of hydrogen-induced compression of the CO adlayer that enhances the dynamic interaction between the adsorbed CO molecules. Note, however, that the dynamic interaction remains weaker than that observed for highest CO coverages in the absence of hydrogen. This indicates that the changes occur in the framework of the surface of a given rhodium particle and no transfer of CO between the metal nanoparticles occurs. As a result, the spectral characteristics of the compressed CO adlayer differ from those of CO monolayer in absence of hydrogen. Thus, the observations in this work clearly show that the repulsive interaction of adsorbed hydrogen with CO adsorbate leads to the compression of CO adlayer on each nanoparticle.

The IR bands of linear CO species observed in the presence of hydrogen adlayer were also deconvoluted into three spectral components (Fig. S4 and S6), where each component was at position that is blue shifted from that registered in the absence of hydrogen. This suggests that all CO molecules that are adsorbed in linear atop configuration at different Rh sites (edges, corners, steps, and face sites) form dense islands separated from the islands formed by absorbed H, probably at (100), (110) and (111) facets.

Under evacuation, the hydrogen adlayer is destroyed as hydrogen desorbs and CO coverage expands back over the all exposed Rh sites on the metal particle. Thus, less dense CO adlayer is formed in which the dipole–dipole interaction between CO molecules is weaker and this reflects in a back red shift in ν(CO).

Conclusions

Rhodium particles obtained by CO reduction of Rh/TiO_2 are highly resistant to CO-induced oxidative disruption: adsorption of CO on the sample at ambient temperature results mainly in the formation of linear Rh^0–CO and bridge–bound carbonyls whereas the amount of $Rh^I(CO)_2$ gem-dicarbonyls is negligible. The position of the carbonyl band due to linear CO species strongly shift to higher frequencies with coverage increases. This shift is due to two effects: dipole-dipole interaction between the adsorbed CO molecules (prevailing at low coverages) and competition of CO adsorbates for electrons donated from the solid (both effects contribute almost equally at high coverages). Adsorption of CO in presence of hydrogen leads to successive occupation of rhodium nanoparticles. However, adsorption of hydrogen on the surface of Rh particles partially pre–covered with CO leads to reversible segregation and compression of the CO adlayer on each rhodium nanoparticle.

Acknowledgements

The authors are indebted to the Union Centre of Excellence (Contract No. DCVP 02-2/2009 with the National Science Fund). The support by the European FP7 project "Beyond Everest" is gratefully acknowledged.

Notes and references

[a] Institute of General and Inorganic Chemistry, Bulgarian Academy of Sciences, Sofia 1113, Bulgaria.
[b] University of Sofia, Department of Chemistry and Pharmacy, Sofia 1126, Bulgaria.
[c] Institute of Mineralogy and Crystallography, Bulgarian Academy of Sciences, Sofia 1113, Bulgaria.

† Electronic Supplementary Information (ESI) available: Figs. S1-S7 and details on CO interaction with single rhodium surfaces. See DOI: 10.1039/b000000x/

1. G. Rupprechter, *Annu. Reports Sec. "C" (Phys. Chem.)*, 2004, **100**, 237-311.
2. A. Föhlisch, M. Nyberg, P. Bennich, L. Triguero, J. Hasselström, O. Karis, L. G. M. Pettersson and A. Nilsson, *J. Chem. Phys.*, 2000, **112**, 1946-1958.
3. K. I. Hadjiivanov and G. N. Vayssilov, *Adv. Catal.*, 2002, **47**, 307-511.
4. R. M. Hammaker, S. A. Francis and R. P. Eischens, *Spectrochim. Acta*, 1965, **21**, 1295-1309.
5. P. Hollins, *Surf. Sci. Rep.*, 1992, **16**, 51-94.
6. C. Ruggiero and P. Hollins, *J. Chem. Soc., Faraday Trans.*, 1996, **92**, 4829-4834.
7. N. Sheppard and T. T. Ngyen, in *Adv. Infrared and Raman Spectros.*, eds. R. J. H. Clark and R. E. Hester, Heyden, London, 1978, vol. 5, pp. 67-148.
8. M. M. Sean, M. Lundwall, F. Yang, Z. Zhou and D. W. Goodman, *J. Phys.: Condens. Matter*, 2009, **21**, 474223.
9. S. D. Worley and C. H. Dai, in *Catalytic Activation of Carbon Dioxide*, American Chemical Society, 1988, vol. 363, pp. 133-146.
10. J. A. Anderson, M. W. McQuire, C. H. Rochester and T. Sweeney, *Catal. Today*, 1991, **9**, 23-30.
11. B. E. Nieuwenhuys, in *Adv. Catal.*, 1999, **44**, 259-328.
12. C. Dujardin, A. S. Mamede, E. Payen, B. Sombret, J. P. Huvenne and P. Granger, *Top. Catal.*, 2004, **30-31**, 347-352.
13. C. C. Miyagawa, J. Kupka and A. Schumpe, *J. Mol. Catal. A: Chem.*, 2005, **234**, 9-17.
14. S. M. McClure, M. J. Lundwall and D. W. Goodman, *Proc. NAS*, 2011, **108**, 931-936.
15. T. M. Apple and C. Dybowski, *J. Catal.*, 1981, **71**, 316-319.
16. B. A. Gurney, L. J. Richter, J. S. Villarrubia and W. Ho, *J. Chem. Phys.*, 1987, **87**, 6710-6721.
17. R. Linke, D. Curulla, M. J. P. Hopstaken and J. W. Niemantsverdriet, *J. Chem. Phys.*, 2001, **115**, 8209-8216.
18. M. M. M. Jansen, J. Gracia, B. E. Nieuwenhuys and J. W. Niemantsverdriet, *Phys. Chem. Chem. Phys.*, 2009, **11**, 10009-10016.

19. I. Nakamura, Y. Kobayashi, H. Hamada and T. Fujitani, *Surf. Sci.*, 2006, **600**, 3235-3242.
20. L. J. Richter, B. A. Gurney and W. Ho, *J. Chem. Phys.*, 1987, **86**, 477-490.
21. M. M. M. Jansen, C. G. M. Hermse and A. P. J. Jansen, *Phys. Chem. Chem. Phys.*, 2010, **12**, 8054-8062.
22. M. M. M. Jansen, O. Caniaz, B. E. Nieuwenhuys and J. W. Niemantsverdriet, *Langmuir*, 2010, **26**, 16239-16245.
23. J. T. Yates Jr, P. A. Thiel and W. H. Weinberg, *Surf. Sci.*, 1979, **84**, 427-439.
24. Y. Kim, H. C. Peebles and J. M. White, *Surf. Sci.*, 1982, **114**, 363-380.
25. E. D. Williams, P. A. Thiel, W. H. Weinberg and J. J. T. Yates, *J. Chem. Phys.*, 1980, **72**, 3496-3505.
26. S. Trautmann and M. Baerns, *J. Catal.*, 1994, **150**, 335-344.
27. H. F. J. Van't Blik, J. B. A. D. Van Zon, T. Huizinga, J. C. Vis, D. C. Koningsberger and R. Prins, *J. Am. Chem. Soc.*, 1985, **107**, 3139-3147.
28. F. Solymosi and M. Pasztor, *J. Phys. Chem.*, 1986, **90**, 5312-5317.
29. P. Basu, D. Panayotov and J. T. Yates, *J. Am. Chem. Soc.*, 1988, **110**, 2074-2081.
30. M. I. Zaki, B. Tesche, L. Kraus and H. Knözinger, *Surf. Interface Anal.*, 1988, **12**, 239-246.
31. M. Frank, R. Kühnemuth, M. Bäumer and H. J. Freund, *Surf. Sci.*, 1999, **427–428**, 288-293.
32. J. Evans, B. Hayden, F. Mosselmans and A. Murray, *Surf. Sci.*, 1992, **279**, L159-L164.
33. F. Solymosi, A. Erdöhelyi and M. Kocsis, *J. Catal.*, 1980, **65**, 428-436.
34. F. Solymosi and M. Pásztor, *J. Catal.*, 1987, **104**, 312-322.
35. S. D. Worley, G. A. Mattson and R. Caudill, *J. Phys. Chem.*, 1983, **87**, 1671-1673.
36. Z. L. Zhang, A. Kladi and X. E. Verykios, *J. Mol. Catal.*, 1994, **89**, 229-246.
37. M. Addamo, V. Augugliaro, A. Di Paola, E. Garcia-Lopez, V. Loddo, G. Marci, R. Molinari, L. Palmisano and M. Schiavello, *J. Phys. Chem. B*, 2004, **108**, 3303-3310.
38. D. A. Buchanan, M. E. Hernandez, F. Solymosi and J. M. White, *J. Catal.*, 1990, **125**, 456-466.
39. M. J. Lundwall, S. M. McClure and D. W. Goodman, *J. Phys. Chem. C*, 2010, **114**, 7904-7912.
40. F. M. Hoffmann, *Surf. Sci. Rep.*, 1983, **3**, 107-107.
41. F. Maugé, C. Binet and J. C. Lavalley, in *Catalysis by Metals*, eds. A. Renouprez and H. Jobic, Springer Berlin Heidelberg, 1997, vol. 6, pp. 1-17.
42. D. A. Panayotov and J. T. Yates Jr, *J. Phys. Chem. C*, 2007, **111**, 2959-2964.
43. K. Hadjiivanov, *J. Chem. Soc. Faraday Trans.*, 1998, **94**, 1901-1904.
44. K. Hadjiivanov, B. M. Reddy and H. Knözinger, *Appl. Catal. A*, 1999, **188**, 355–360.
45. R. M. Hammaker, S. A. Francis and R. P. Eischens, *Spectrochim. Acta*, 1965, **21**, 1295.
46. R. K. Brandt, M. R. Hughes, L. P. Bourget, K. Truszkowska and R. G. Greenler, *Surf. Sci.*, 1993, **286**, 15-25.
47. M. Fukuoka, M. Okada, M. Matsumoto, S. Ogura, K. Fukutani and T. Kasai, *Phys. Rev. B*, 2007, **75**, 235434.
48. J. C. Conesa and J. Soria, *J. Phys. Chem.*, 1982, **86**, 1392-1395.
49. L. J. Richter, T. A. Germer and W. Ho, *Surf. Sci.*, 1988, **195**, L182-L192.

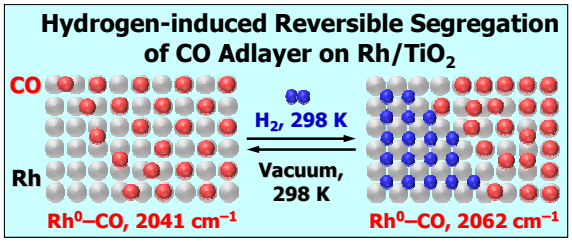

Adsorption of hydrogen on titania-supported Rh nanoparticles partially covered by CO causes compression of the CO adlayer.